Supplementary Information

Effects of cigarette smoke, cessation and switching to two heat-not-burn tobacco products on lung lipid metabolism in *C57BL/6* and *Apoe*^{-/-} mice – an integrative systems toxicology analysis

Bjoern Titz[a,*], Stéphanie Boué[a,*], Blaine Phillips[b], Marja Talikka[a], Terhi Vihervaara[c], Thomas Schneider[a], Catherine Nury[a], Ashraf Elamin[a], Emmanuel Guedj[a], Michael J. Peck[a], Walter K. Schlage[a], Maciej Cabanski[a,d], Patrice Leroy[a], Gregory Vuillaume[a], Florian Martin[a], Nikolai V. Ivanov[a], Emilija Veljkovic[a], Kim Ekroos[c], Reijo Laaksonen[c], Patrick Vanscheeuwijck[a], Manuel C. Peitsch[a], Julia Hoeng[a].

[a] Philip Morris International Research and Development, Quai Jeanrenaud 5, 2000 Neuchatel, Switzerland

[b] Philip Morris International Research Laboratories, 50 Science Park Road, Singapore, Singapore

[c] Zora Biosciences Oy, Biologinkuja 1, 02150 Espoo, Finland

[d] Current address for MC: Novartis Pharma AG, Novartis

[*] SB and BT contributed equally to this manuscript.

Corresponding author:

Julia Hoeng, Ph.D MBA

E-mail: julia.hoeng@pmi.com

Tel: +41 (58) 242 2214

Running Title: Cigarette smoke affects lung lipid metabolism

Extended Materials and Methods

In this integrative systems toxicology analysis we focus on alterations related to lung lipid metabolism for C57BL/6 and Apoe-/- mice exposed to cigarette smoke (CS), potential MRTP aerosols, or CS-exposed mice that underwent cessation or switching to the MRTP. This analysis is part of two larger systems toxicology assessment studies, which are described in more detail elsewhere ((Phillips et al., 2015) and this issue). For a high level summary of the proteomics results, the reader is referred to these publications. The lung lipidomics data are specific to this manuscript and to provide the full context of this integrative analysis, we have summarized all relevant Materials and Methods for the studies in both mouse strains below.

General Study Design

Apoe$^{-/-}$ study. Female Apoe$-/-$ mice were randomized into five groups: (i) sham (exposed to air), (ii) 3R4F (exposed to CS from the reference cigarette 3R4F), (iii) THS2.2 (exposed to mainstream aerosol from THS2.2 at nicotine levels matched to those of 3R4F), (iv) smoking cessation, and (v) switching to THS2.2. Mice from the sham, 3R4F, and THS2.2 groups were exposed to fresh air, CS from 3R4F, or THS2.2 aerosol, respectively, for up to 8 months. To model effects of smoking cessation and switching to THS2.2, mice from the cessation and switching groups were first exposed to 3R4F for 2 months and then switched to air or THS2.2 aerosol, respectively, for up to 6 additional months (Fig. 1A). Female mice were chosen because of their proposed increased susceptibility to emphysema (Bartalesi et al., 2005).

C57BL/6 study. Female C57BL/6 mice were randomized into five groups: (i) sham (exposed to air), (ii) 3R4F (exposed to CS from the reference cigarette 3R4F), (iii) pMRTP (exposed to mainstream aerosol from pMRTP at nicotine levels matched to those of 3R4F), (iv) smoking cessation, and (v) switching to pMRTP. Mice from the sham, 3R4F, and pMRTP groups were exposed to fresh air, CS from 3R4F, or pMRTP aerosol, respectively, for up to 7 months. To model effects of smoking cessation and switching to pMRTP, mice from the cessation and switching groups were first exposed to 3R4F for 2

months and then switched to air or pMRTP aerosol, respectively, for up to 5 additional months (Fig. 1A).

Reference Cigarettes and potential MRTPs

3R4F cigarettes were purchased from the University of Kentucky (Lexington, KY, USA, http://www.ca.uky.edu/refcig). The pMRTP (provided in seven batches by Philip Morris Products S.A., Neuchâtel, Switzerland; all produced in 2012) has a carbon tip attached to a column of tobacco filler that serves as a fast-lighting heat source to generate an aerosol containing water, glycerin, nicotine and volatiles contributing to tobacco flavors. This technology, by avoiding tobacco combustion, reduces formation of HPHCs. The type of pMRTP used throughout this study was not identical to that used in a previously published 28-day rat inhalation study (Kogel et al., 2014). The candidate MRTP, THS2.2, consists of a stick containing a tobacco plug inserted into a holder that electrically heats the tobacco in a controlled way to ensure combustion temperatures are not reached. This process generates an aerosol containing mainly water, glycerin, nicotine, and volatiles contributing to tobacco flavors. THS2.2 sticks were produced at Philip Morris International (PMI; Neuchâtel, Switzerland) in three batches. In the smoking system, the THS2.2 stick was inserted into a cigarette holder that heats the tobacco plug. The cigarette holder included a battery, electronics for controlling, a heating element, and the cigarette extractor. Cigarette holders were provided by PMI.

Comparative analytical specifications of the pMRTP aerosol, THS2.2 aerosol, and 3R4F CS yields are given in Supplementary Table 1, which shows the quantification of 56 HPHCs plus water and glycerol (as a humectant) in a total of 58 analytes from 3R4F CS and THS2.2 aerosol. In the Table, the concentrations of these analytes are normalized to that of nicotine.

Mainstream CS from 3R4F cigarettes was generated on 30-port rotary smoking machines (type PMRL-G, SM2000) as described previously (Phillips et al., 2015). Aerosols from THS2.2 sticks were generated on modified 30-port rotary smoking machines equipped with the appropriate holders. Two modified smoking machines per chamber were required to achieve the target THS2.2 aerosol concentration. pMRTP aerosol was generated in modified SM2000 machines.

3

3R4F cigarettes, THS2.2 sticks, and pMRTP sticks were smoked according to the Health Canada Intensive Smoking Protocol based on ISO standard 3308 (revised in 2000), with the exception of the puff volume (55 ml) and puff frequency (one puff every 30 s) as described previously (Phillips et al., 2015). Several additional minor deviations from ISO standard 3308 were necessary for technical reasons (Supplementary Table 2).

Mice and Inhalation Exposures

All procedures involving animals were performed in an Association for Assessment and Accreditation of Laboratory Animal Care International-accredited, Agri-Food & Veterinary Authority of Singapore-licensed facility with approval from an Institutional Animal Care and Use Committee (IACUC protocol #15015). This was in compliance with the National Advisory Committee for Laboratory Animal Research Guidelines on the Care and Use of Animals for Scientific Purposes (NACLAR, 2004).

Female B6.129P2-Apoe (tm1Unc)N11 (Apoe$^{-/-}$) mice bred under specific pathogen-free conditions were obtained from Taconic Biosciences (Germantown, NY, USA). The mice were approximately 6–8 wk old on arrival and 8–10 wk old at the start of the exposure. Their health status on arrival was verified using the health check certificate provided by the breeder. Additional health checks on tissue samples collected in Singapore were performed at Harlan Laboratories (Derby, UK). Female C57BL/6 mice bred under specific pathogen-free conditions were obtained from Charles River (Wilmington, MA, USA) and were 8–10 wk old at exposure initiation. Mice were individually identified by subcutaneous transponders and were housed and whole-body exposed in the animal laboratory under specific pathogen-free conditions. Random assignment of mice to experimental groups was conducted prior to exposure using a randomization sequence stratified by body weight. A maximum of eight mice were housed per cage. Cage-enrichment (Igloo™, Biosy, Malaysia, and Nylabone™, Neptune City, NJ, USA) was provided in each cage during the non-exposure periods. The bedding material (Lignocel®BK 8-15, J. Rettenmaier & Soehne, GmbH & Co KG., Rosenberg, Germany) was composed of autoclaved softwood (fur and spruce) granulate. A gamma-irradiated pellet diet (T2914C rodent diet, Harlan Laboratories) was provided. Filtered tap water was supplied ad libitum and changed daily. Diet was

4

unavailable only during the exposure periods, but the animals had constant access to drinking water. Additional details of animal housing, randomization, and acclimatization are described in our previous reports ((Phillips et al., 2015) and manuscript submitted).

C57BL/6 mice were whole body-exposed to diluted mainstream smoke from 3R4F (750 mg TPM/m3, equivalent to 34.4 µg nicotine/l), pMRTP aerosol (nicotine-matched to 3R4F, 34.4 mg/ m3) or filtered air for 4 h per day, 5 days per wk, for up to 7 months. Mice exposed to air served as the control (sham) group.

The Apoe$^{-/-}$ mice were whole body-exposed to diluted mainstream smoke from 3R4F (600 mg TPM/m3, equivalent to 29.9 µg nicotine/l), THS2.2 aerosol (nicotine-matched to 3R4F, 29.9 mg/ m3) or filtered air for 3 h per day, 5 days per wk, for up to 8 months, with intermittent daily exposure to fresh filtered air for 30 min after the first h of smoke exposure and for 60 min after the second h of exposure. This was done to avoid a build-up of excessive carboxyhemoglobin (COHb) concentrations in the 3R4F group. For the sham group, mice were exposed only to air.

The atmosphere in the aerosol exposure chambers was monitored as previously described (Phillips et al., 2015). Briefly, flow rate, temperature, relative humidity and carbon monoxide (CO) were monitored continuously; TPM (gravimetric evaluation of TPM collected on Cambridge filters), nicotine (LC evaluation of nicotine trapped on sulphuric acid acidified Extrelut® 3NT column) and static puff volume measurements were taken daily; formaldehyde, acetaldehyde, and acrolein (LC evaluation of aldehydes collected and converted to hydrazine derivatives in 2,4 DNPH trapping solution) measurements were taken at least weekly; and particle size distribution was determined at least once per mo.

Animals were observed on a daily basis, body weight progression was monitored weekly, and exposure parameters (COHb in blood and nicotine metabolites in urine) were measured three times during the study. For a more detailed description of the procedures, see (Phillips et al., 2015).

5

Lipidomics

Samples. Lipidomics samples were analyzed after 2, 3, and 7 months exposure in the C57BL/6 and for the 2, 3, and 8 months exposure in the Apoe^{-/-} study. For each exposure group, lung tissue samples from eight mice, providing eight biological replicates, were analyzed. Lungs were perfused through the right ventricle with a 27-G needle delivering ice-cold 0.9% physiological saline to remove contaminating blood cells. Tissue samples were pulverized with a CP02 CryoPrep Dry Pulverization System (Covaris, Woburn, MA,USA) and samples, at a concentration of 100 mg/ml, were homogenized in ice-cold 70% methanol-H_2O containing 0.1% butyl-hydroxy-toluene (BHT). Homogenized samples were stored at -80°C prior to lipid extraction and analysis. All lipidomics analyses were performed by Zora Biosciences Oy (Espoo, Finland).

Lipid extraction. Robotic assisted 96-well sample preparation and extraction was performed using a Hamilton Microlab Star system (Hamilton Robotics, Bonaduz, Switzerland). A modified Folch protocol, using chloroform, methanol and acetic acid for liquid-liquid extraction (Heiskanen et al., 2013), was applied to extract a broad lipid type spectrum (Folch et al., 1957, Stahlman et al., 2009). This extraction procedure is efficient and robust over a wide range of lipid concentrations (Iverson et al., 2001). This method was used to extract glycerolipids, glycerophospholipids, sterol esters and sphingolipids, except for sphingosines and spingosine-1-phosphates which were extracted with 1.1 mL of ice-cold methanol containing 0.1% BHT. The Hamilton robot system was used to extract gangliosides using the methodology described by Fong and colleagues (Fong et al., 2009) with minor modifications. Eicosanoids were extracted according to the procedure by Deems (Deems et al., 2007). Prior to extraction, the samples were spiked with known amounts of internal standards (IS). This set of ISs was used to quantify endogenous lipids in samples and controls as described below. Following lipid extraction, samples were dried under a gentle stream of nitrogen. Samples for shotgun lipidomics, sphingolipidomics and gangliosides were reconstituted in chloroform:methanol (1:2, v/v), whereas samples for sphingosine/sphingosine-1-phosphate and eicosanoids were reconstituted in methanol. The final extracts were stored at −20°C prior to mass spectrometry analysis.

6

Shotgun Lipidomics. Quantification of molecular glycerolipids, glycerophospholipids and sterol esters was assessed by shotgun lipidomics as previously described (Heiskanen et al., 2013). Samples were loaded into 96-well plates (twin.tec PCR Plate 96, Eppendorf AG, Hamburg, Germany) and sealed with an aluminum foil (Heatsealing Foil, Eppendorf AG). Aliquots of 10 µL were aspirated and infused. Precursor ion and neutral loss scans were carried out in positive and negative ion modes, as described previously (Ekroos et al., 2002, Ekroos et al., 2003, Liebisch et al., 2006). On the TriVersa NanoMate electrospray ionization (ESI) voltages applied were typically 1.3 kV and -1.3 kV in positive and negative ion modes, respectively. Gas pressure was typically set to 0.75 psi in both polarity modes. In the positive ion mode the following MS settings were used: curtain gas; 20, collision gas; 6, interface heater; 60, declustering potential; 30, entrance potential 10 and collision cell exit potential; 20. In negative ion mode the following settings were used: curtain gas; 20, collision gas; 6, interface heater; 60, declustering potential; -100, entrance potential -10 and collision cell exit potential; -20. Q1 and Q3 quadrupoles were operated in unit resolution mode.

Sphingolipidomics. Molecular ceramides, glucosylceramides, lactosylceramides and globotriaosylceramides were analyzed as previously described (Merrill et al., 2005). Briefly, individual species were separated on an Acquity BEH C18, 2.1×50 mm column with a particle size of 1.7 µm (Waters, Milford, MA, USA) assessed on a UHPLC system comprising of a CTC HTC PAL autosampler (CTC Analytics AG, Zwingen, Switzerland) and a Rheos Allegro pump (Flux Instruments, Reinach, Switzerland). A 25 min gradient using 10 mM ammonium acetate in water with 0.1% formic acid (mobile phase A) and 10 mM ammonium acetate in acetonitrile:2-propanol (4:3, v/v) containing 0.1% formic acid (mobile phase B) was used. The column oven temperature was set to 60 °C and a flow rate was 500 µL/min. Final lipid extracts,10 µL aliquots each, were injected. A QTRAP 5500 mass spectrometer (Sciex, Concord, Canada) equipped with an electrospray ion source was used for mass spectrometric determination. The instrument was operated in multiple reaction monitoring (MRM) mode in positive ion mode as previously described (Merrill et al., 2005). 78 MRM transitions were monitored using a dwell time of 20 ms. Q1 and Q3 quadrupoles were operated in unit resolution mode. The collision energy was set at 40 eV for ceramides, 45 eV for glucosyl- and lactosylceramides and 66

eV for globotriaosylceramides. Nitrogen was used as collision gas. ESI voltage was set at 5000 V and the ion source temperature at 400 °C.

Sphingosines and sphingosine-1-phosphates were analyzed on a similar system to that described above. Individual species were separated on an AQUASIL C18, 2.1 x 50 mm column with a particle size of 5 µm (Thermo Fisher Scientific, San Jose, USA). A 19 min gradient using 5 mM ammonium acetate in ultra-pure water (UPW):methanol (1:1) with 0.1% formic acid (mobile phase A), 5 mM ammonium acetate in methanol with 0.1% formic acid (mobile phase B) and 10 mM ammonium acetate in isopropanol with 0.1% formic acid (mobile phase C) was used. The column oven temperature was set to 60 °C and the flow rate was 750 µL/min. Final lipid extracts, 10 µL aliquots each, were injected. The individual species were monitored in MRM mode in positive ion mode. 22 MRM transitions were monitored using a dwell time of 25 ms. Q1 and Q3 quadrupoles were operated in unit resolution mode. The collision energy was set at 22 eV for sphingosines and 21 eV for sphingosine-1-phosphates. Nitrogen was used as collision gas. ESI voltage was set at 4500 V and ion source temperature at 550 °C. Ganglioside lipidomics. Gangliosides were analyzed as described previously (Ikeda et al., 2008) except that 10 mM ammonium acetate and 0.1% formic acid were used in all solvents instead of ammonium formate. The analysis was assessed on a 4000 QTRAP (Sciex, Concord, Canada) equipped with a similar UHPLC system as described above. Individual species were separated on an Acquity BEH C18, 2.1 × 50 mm column with a particle size of 1.7 µm (Waters, Milford, MA, USA). A 32 min gradient using 10 mM ammonium acetate in methanol with 0.1% formic acid (mobile phase A), 10 mM ammonium acetate in isopropanol with 0.1% formic acid (mobile phase B) and 10 mM ammonium acetate in HPLC grade water with 0.1% formic acid (mobile phase C) was used. The column oven temperature was set to 45 °C and the flow rate was 500 µL/min. Final lipid extracts, 10 µL aliquots of each, were injected. Individual species were monitored in MRM mode in negative ion mode. 103 MRM transitions were monitored using a dwell time of 30 ms. Q1 and Q3 quadrupoles were operated in unit resolution mode. Collision energy was set at 90 eV for GM3s, 80 eV for GM2s, 70 eV for GM1s and 60 eV for GQs, GTs, and GDs. Nitrogen was used as collision gas. ESI voltage was set at -4500 V and ion source temperature at 400 °C.

Eicosanoid lipidomics. Eicosanoids were analyzed as described previously (Deems et al., 2007). A similar instrument arrangement was used as for sphingolipidomics. Individual species were separated on a Phenomenex Jupiter, 250 × 2.0 mm column with a particle size of 5 µm (Phenomenex, Torrance, CA, USA). A 18 min gradient using water:acetonitrile:formic acid (63:37:0.02) (mobile phase A) and acetonitrile:isopropanol (50:50) (mobile phase B) was used. The column oven temperature was set to 60 °C and the flow rate was 300 µL/min. Final lipid extracts, 10 µL aliquots of each, were injected. Individual species were monitored in MRM mode in negative ion mode. 103 MRM transitions, split in two runs, were monitored using a dwell time of 15 ms. Q1 and Q3 quadrupoles were operated in unit resolution mode. Collision energy was set according to Deems and colleagues (Deems et al., 2007). Nitrogen was used as collision gas. ESI voltage was set at -4500 V and ion source temperature at 525 °C.

Lipid identification and quantification. Mass spectrometry data files were processed using LipidView™ V1.0.99 and MultiQuant™ 2.0 software to generate a list of lipid names and peak areas. Shotgun lipidomics data were processed in LipidView™ as described previously (Ejsing et al., 2006). Briefly, endogenous species were identified based on their characteristic fragment ions, neutral losses and parent ions. For instance, m/z 184.1 which is the characteristic headgroup ion of phosphatidylcholines (PC) and sphingomyelins (SM) (Brugger et al., 1997) was used to identify together with the parent mass the peaks observed in the mass spectrum of PIS 184.1 in positive ion mode. In a similar way the monitored acyl ions were utilized to identify the molecular species in negative ion mode (Ekroos et al., 2003). For instance, identification of PC 16:0-18:1 requires corresponding signals from both the 16:0 (PIS of m/z 255.2) and the 18:1 (PIS of m/z 281.2) scans.

MRM data were processed in MultiQuant™. Selected lipid characteristic ions and their parent masses in conjunction with retention time were used for identification of the endogenous species. Information dependent acquisition (IDA) experiments were used for confirming identifications. MRM was used as survey scan to trigger the IDA, followed by enhanced product ion (EPI) scans of the two most intense ions.

9

The identified lipids were quantified by normalizing against their respective internal standard and matrix type.

Data filtering of the final data set was based on the frequency of individual lipid molecules observed throughout the collected data. Molecules observed from fewer than 75% of samples, and molecules lacking lipid class specific internal standards were excluded. Any molecule having fourfold lower or higher concentration than the median of the group was considered an outlier and excluded. Filtering procedures were performed separately for both polarity modes and lipidomic assessment, prior to merging of the final lipidomic data set. All calculations and data processing were performed with SAS 9.3 software (SAS Institute, Cary, NC, USA).

Quality control. To ascertain data quality, various controls were assessed. Data that fulfilled all applied acceptance criteria were accepted. In all analyses, instrument controls (IC), quality controls (QC), blanks and calibration lines were applied. ICs were based on pooled extracts from fresh human plasma analyzed in a similar manner as were the samples. The ICs served to monitor performance and variation in the mass spectrometry analyses (Heiskanen et al., 2013). Depending on the analysis and molecular abundance different thresholds were applied, but were typically in the range of 20-50%. The samples were run again if thresholds were exceeded. QCs served in the same way as ICs, except that the sample matrix, if available, was the same as that of the samples to be analyzed, and they were individually extracted to enable assessment of extraction efficiency. Compared with for ICs, thresholds of slightly greater variation were typically applied for QCs. Blanks served to monitor background noise and if the signal of a lipid molecule exceeded 25% in the blank it was excluded. Calibration lines served to monitor the linear response of the mass spectrometer. The analysis was accepted based on the linearity of the calibration lines. The linear regression was required to exceed 0.95 based on at least four out of six non-zero standards.

Data analysis and differential abundance. Outlier samples with low total concentrations of all measured lipids were excluded. Samples with total lipid concentrations 1.5 interquartile ranges (IQRs) below the first quartile were defined as outliers. With this, the animal numbers (CAN) 920104 and

10

920660 were excluded for the Apoe$^{-/-}$ study but all samples of the C57BL/6 study were retained. For global comparison of lipid class concentrations between the two studies, median concentrations of the lipid species were calculated and summed for all lipid species of a class. The "species fractions" represent the relative molar contribution of a given lipid species to the total measured concentration of its class, e.g. the contribution of PC 16:0/16:0 to all PC lipids. These "species fractions" were calculated as the median concentration of the lipid species divided by the sum of all median concentrations of its lipid class. The differential abundance analysis was conducted separately for exposure time point in each study. In each comparison between a given exposure group and the respective sham group only lipid species detected in at least 50% of the samples of each compared group were considered. The log2 fold-change relative to corresponding levels in the sham exposure group was calculated. A t-test was used to estimate the statistical significance and within each comparison the obtained p-values were corrected for multiple hypothesis testing using the Benjamini-Hochberg (BH) approach. Abundance differences of lipid species with a BH-adjusted p-value < 0.05 were considered as statistically significant.

Proteomics

Sample preparation for LC-MS based proteomics in the C57BL/6 study. Lung tissue samples from six mice, providing six biological replicates, were analyzed for each exposure condition and time point. Lung tissue samples from months 1, 3, 5, and 7 for 3R4F and pMRTP exposures and months 3, 5, and 7 for cessation and switch were available for quantitative proteomic analysis. The right lung was cryo-sectioned into 20 μm slices. The slices were homogenized with a bead-assisted procedure in Tissue Lyser II (Qiagen, Valencia, CA, USA) in tissue lysis buffer (BioRad, Hercules, CA, USA) and the proteins precipitated with acetone. The precipitate was resuspended in 0.5 M triethylammonium bicarbonate (TEAB, Sigma-Aldrich, St. Louis, MO, USA), 1M urea (Sigma-Aldrich) and 0.1% SDS (Sigma-Aldrich). A 50 μg aliquot was processed for iTRAQ 8-plex labeling procedure according to the manufacturer's instructions (AB Sciex, Framingham, MA, USA). Trypsin (Promega, Madison, WI, USA) was added to samples at a 1:10 trypsin to protein ratio (w/w) followed by overnight digestion at

11

37°C. Trypsin-digested samples were labeled with reporter-ion tags for the appropriate treatment group. In addition, a common reference mix containing 50 µg of all protein extracts from each time point was prepared and labeled with iTRAQ reporter-ion tag. All labeled samples belonging to one iTRAQ set were pooled and dried in a SpeedVac. Samples were desalted with 1 cc C18 reversed phase SepPak columns (Waters, Milford, MA, USA) and 0.5 ml bed volume detergent removal columns (Pierce, Rockford, IL, USA) according to the manufacturers' instructions. Samples were dried in the SpeedVac and resuspended in nanoLC buffer A (5% acetonitrile (Sigma-Aldrich), 0.2% formic acid (Sigma-Aldrich).

Sample preparation for LC-MS based proteomics in the Apoe-/- study. Tissue samples from the right lungs of eight mice, providing eight biological replicates, were analyzed for each exposure condition and time point. Right lung tissue samples from months 1, 2, 3, 6, and 8 for 3R4F and THS 2.2 exposures and months 3, 6, and 8 for cessation and switching (to THS 2.2) were available for quantitative proteomic analysis. All samples were processed in random order. Frozen right lung tissue was homogenized with a bead-assisted procedure in Tissue Lyser II (Qiagen, Valencia, CA, USA) in tissue lysis buffer (BioRad). After lysis proteins were precipitated in acetone. The precipitate was resuspended in 0.5 M triethylammonium bicarbonate (TEAB, Sigma-Aldrich), 1M urea (Sigma-Aldrich) and 0.1% SDS (Sigma-Aldrich). Aliquots of 50 µg were processed for the TMT 6-plex labeling procedure according to the manufacturer's instructions (Thermo Scientific, USA). Trypsin (Promega) was added to samples at a 1:10 trypsin to protein ratio (w/w) followed by overnight digestion at 37°C. Trypsin-digested samples were labeled with reporter-ion tags for the appropriate treatment groups. In addition, a common reference mix containing 50 µg of all protein extracts from each time point was prepared and labeled with a TMT reporter-ion tag. For each mo of exposure eight replicate TMT 6-plex sets with the five different exposure groups and the reference mix were defined. Within each mo, replicates were randomly assigned to the TMT sets and the sample-to-reporter mapping was randomized within each set. All labeled samples of one TMT set were pooled and dried in a SpeedVac. Samples were purified from SDS and remaining salts with 0.5 ml bed volume detergent removal columns (Pierce) and 1 cc C18 reversed phase SepPak columns (Waters) according to the manufacturers' instructions, followed

12

by drying in a Speedvac and resuspension in nanoLC buffer A (5% acetonitrile (Sigma-Aldrich), 0.2% formic acid (Sigma-Aldrich).

Mass-spectrometry for identification and quantification in the C57BL/6 study. Samples were analyzed using an Easy nanoLC 1000 instrument connected online to a Q-Exactive (Thermo Scientific, Waltham, MA, USA) mass-analyzer. Peptides were fractionated on a 50 cm long C18RP RSLC Easyspray column (2 µm particle size; Thermo Scientific) at a flow rate of 200 nl/min with a 200 min gradient from nanoLC buffer A (5% acetonitrile, 0.2% formic acid) to 40% acetonitrile, 0.2% formic acid. Each sample was injected twice with 2 different analysis methods. Mass-spectrometry data were searched against the mouse reference proteome set (Uniprot, version Aug_2013,) using Proteome Discoverer vers. 1.4.0.288 software (Thermo Scientific). Mascot (v.2.3, Matrixscience, Boston, MA, USA) and SequestHT were used as search tools and resulting protein lists were merged and iTRAQ-reporter ion intensities were determined from the Proteome Discoverer software. Peptide identification probability had to be $\geq$ 95%. The Percolator node of the Proteome Discoverer software was used to estimate peptide-level adjusted p-values (q-values) and the peptides were filtered for a q-value < 0.05 (i.e., the false discovery rate was controlled at the 5% level). The quantification of iTRAQ reporter ions and the peptide to protein (group) assignments was performed with the Proteome Discoverer software. iTRAQ peptide-level quantification data was exported and further processed in the R statistical environment (R Development Core Team, 2007). The quantification data were filtered for "unique" quantification results as defined by the Proteome Discoverer software, for example, to remove redundant quantification results from multiple search engines. A global variance stabilizing normalization (VSN) was performed with the respective Bioconductor package in R (Huber et al., 2002; Karp et al., 2010). Each iTRAQ reporter ion set was normalized to its median and protein expression values were calculated as the median of these normalized peptide-level quantification values (Herbrich et al., 2013). A linear model was fit for each exposure condition and its respective sham group and p-values from a moderated t-statistics were calculated with the empirical Bayes approach (Gentleman et al., 2004). The Benjamini-Hochberg False Discovery Rate (FDR) method was then used to correct for multiple testing effects. Proteins with an adjusted p-value < 0.05 were considered as differentially expressed.

13

Mass-spectrometry for identification and quantification in the Apoe-/- study. Samples were analyzed in random order using an Easy nanoLC 1000 instrument (Thermo Scientific) connected online to a Q-Exactive (Thermo Scientific) mass-analyzer. Peptides were fractionated on a 50 cm C18RP RSLC Easyspray column (2 μm particle size; Thermo Scientific) at a flow rate of 200 nl/min with a 200 min gradient from nanoLC buffer A (5% acetonitrile, 0.2% formic acid) to 40% acetonitrile, 0.2% formic acid. Each sample was injected twice with 2 different analysis methods: a fast and a sensitive method as described by Kelstrup et al. (Kelstrup et al., 2012) on the same column. Both mass-spectrometry runs were searched together as merged mass-lists against the mouse reference proteome set (Uniprot, version July 2014, canonical isoforms only) using Proteome Discoverer vers. 1.4.0.288 software (Thermo Scientific). Mascot (v.2.4.1, Matrixscience) and SequestHT (implemented in Proteome Discoverer) were used as search tools and resulting protein lists were merged and TMT-reporter ion intensities were determined from the Proteome Discoverer software. The Percolator node of the Proteome Discoverer software was used to estimate peptide-level adjusted p-values (q-values) and the peptides were filtered for a q-value < 0.05 (that is, the false discovery rate was controlled at the 5% level). TMT peptide-level quantification data was exported and further processed in the R statistical environment (R Development Core Team, 2007). The quantification data were filtered for "unique" quantification results as defined by the Proteome Discoverer software, for example, to remove redundant quantification results from multiple search engines. A global variance stabilizing normalization (VSN) was performed with the respective Bioconductor package in R (Huber et al., 2002, Karp et al., 2010). Each TMT reporter ion set was normalized to its median and protein expression values were calculated as the median of these normalized peptide-level quantification values (Herbrich et al., 2013). For the detection of differentially expressed proteins, a linear model was fit for each exposure condition and its respective sham group and p-values from a moderated t-statistics were calculated with the empirical Bayes approach (Gentleman et al., 2004). The Benjamini-Hochberg False Discovery Rate (FDR) method was then used to correct for multiple testing effects. Proteins with an adjusted p-value < 0.05 were considered as differentially expressed.

14

Additional data analysis methods

Protein set analysis was supported by the Piano package in the R statistical environment (Väremo et al., 2013). Lipid pathway maps were obtained from the KEGG database (Kanehisa et al., 2014). The $\log_2$ fold-change was used as the protein statistic, the mean as the set statistic and sample permutation within the group comparisons and p-value adjustment with the Benjamini-Hochberg procedure were used to estimate statistical significances. Visualization of lipid and protein abundance differences on KEGG pathway maps was supported by the Pathview package in R (Luo and Brouwer, 2013).

The sparse partial least squares (sPLS) approach was conducted in the canonical mode with the mixOmics package in R (Lê Cao et al., 2009). For the proteomics data, 100 variables were kept in the loadings and 50 variables were kept for the lipidomics data. The analysis of transcription factor activities and the network perturbation amplitude analysis for the Nfe2l2 signaling network were based on transcriptomics measurements (Phillips et al., 2015) and performed as described, previously (Martin et al., 2014, Martin et al., 2012).

References

Brugger B., Erben G., Sandhoff R., Wieland F. T., and Lehmann W. D. (1997). Quantitative analysis of biological membrane lipids at the low picomole level by nano-electrospray ionization tandem mass spectrometry. Proc Natl Acad Sci U S A **94**, 2339-2344.

Deems R., Buczynski M. W., Bowers-Gentry R., Harkewicz R., and Dennis E. A. (2007). Detection and quantitation of eicosanoids via high performance liquid chromatography-electrospray ionization-mass spectrometry. Methods Enzymol **432**, 59-82.

Ejsing C. S., Duchoslav E., Sampaio J., Simons K., Bonner R., Thiele C., Ekroos K., and Shevchenko A. (2006). Automated identification and quantification of glycerophospholipid molecular species by multiple precursor ion scanning. Anal Chem **78**, 6202-6214.

Ekroos K., Chernushevich I. V., Simons K., and Shevchenko A. (2002). Quantitative profiling of phospholipids by multiple precursor ion scanning on a hybrid quadrupole time-of-flight mass spectrometer. Anal Chem **74**, 941-949.

Ekroos K., Ejsing C. S., Bahr U., Karas M., Simons K., and Shevchenko A. (2003). Charting molecular composition of phosphatidylcholines by fatty acid scanning and ion trap MS3 fragmentation. J Lipid Res **44**, 2181-2192.

Folch J., Lees M., and Sloane Stanley G. H. (1957). A simple method for the isolation and purification of total lipides from animal tissues. J Biol Chem **226**, 497-509.

Fong B., Norris C., Lowe E., and McJarrow P. (2009). Liquid chromatography-high-resolution mass spectrometry for quantitative analysis of gangliosides. Lipids **44**, 867-874.

Heiskanen L. A., Suoniemi M., Ta H. X., Tarasov K., and Ekroos K. (2013). Long-term performance and stability of molecular shotgun lipidomic analysis of human plasma samples. Anal Chem **85**, 8757-8763.

Ikeda K., Shimizu T., and Taguchi R. (2008). Targeted analysis of ganglioside and sulfatide molecular species by LC/ESI-MS/MS with theoretically expanded multiple reaction monitoring. J Lipid Res **49**, 2678-2689.

Iverson S. J., Lang S. L., and Cooper M. H. (2001). Comparison of the Bligh and Dyer and Folch methods for total lipid determination in a broad range of marine tissue. Lipids **36**, 1283-1287.

Kanehisa M., Goto S., Sato Y., Kawashima M., Furumichi M., and Tanabe M. (2014). Data, information, knowledge and principle: back to metabolism in KEGG. Nucleic acids research **42**, D199-D205.

Kogel U., Schlage W. K., Martin F., Xiang Y., Ansari S., Leroy P., Vanscheeuwijck P., Gebel S., Buettner A., and Wyss C. (2014). A 28-day rat inhalation study with an integrated

molecular toxicology endpoint demonstrates reduced exposure effects for a prototypic modified risk tobacco product compared with conventional cigarettes. Food and Chemical Toxicology **68**, 204-217.

Lê Cao K.-A., González I., and Déjean S. (2009). integrOmics: an R package to unravel relationships between two omics datasets. Bioinformatics **25**, 2855-2856.

Liebisch G., Binder M., Schifferer R., Langmann T., Schulz B., and Schmitz G. (2006). High throughput quantification of cholesterol and cholesteryl ester by electrospray ionization tandem mass spectrometry (ESI-MS/MS). Biochim Biophys Acta **1761**, 121-128.

Luo W., and Brouwer C. (2013). Pathview: an R/Bioconductor package for pathway-based data integration and visualization. Bioinformatics **29**, 1830-1831.

Martin F., Sewer A., Talikka M., Xiang Y., Hoeng J., and Peitsch M. C. (2014). Quantification of biological network perturbations for mechanistic insight and diagnostics using two-layer causal models. BMC Bioinformatics **15**, 238.

Martin F., Thomson T. M., Sewer A., Drubin D. A., Mathis C., Weisensee D., Pratt D., Hoeng J., and Peitsch M. C. (2012). Assessment of network perturbation amplitudes by applying high-throughput data to causal biological networks. BMC systems biology **6**, 54.

Merrill A. H., Jr., Sullards M. C., Allegood J. C., Kelly S., and Wang E. (2005). Sphingolipidomics: high-throughput, structure-specific, and quantitative analysis of sphingolipids by liquid chromatography tandem mass spectrometry. Methods **36**, 207-224.

Phillips B., Veljkovic E., Peck M. J., Buettner A., Elamin A., Guedj E., Vuillaume G., Ivanov N. V., Martin F., Boue S., Schlage W. K., Schneider T., Titz B., Talikka M., Vanscheeuwijck P., Hoeng J., and Peitsch M. C. (2015). A 7-month cigarette smoke inhalation study in C57BL/6 mice demonstrates reduced lung inflammation and emphysema following smoking cessation or aerosol exposure from a prototypic modified risk tobacco product. Food Chem Toxicol **80**, 328-345.

Rustemeier K., Demetriou D., Schepers G., and Voncken P. (1993). High-performance liquid chromatographic determination of nicotine and its urinary metabolites via their 1,3-diethyl-2-thiobarbituric acid derivatives. J Chromatogr **613**, 95-103.

Stahlman M., Ejsing C. S., Tarasov K., Perman J., Boren J., and Ekroos K. (2009). High-throughput shotgun lipidomics by quadrupole time-of-flight mass spectrometry. J Chromatogr B Analyt Technol Biomed Life Sci **877**, 2664-2672.

Terpstra P. M., Teredesai A., Vanscheeuwijck P. M., Verbeeck J., Schepers G., Radtke F., Kuhl P., Gomm W., Anskeit E., and Patskan G. (2003). Toxicological evaluation of an electrically heated cigarette. Part 4: Subchronic inhalation toxicology. Journal of applied toxicology **23**, 349-362.

Väremo L., Nielsen J., and Nookaew I. (2013). Enriching the gene set analysis of genome-wide data by incorporating directionality of gene expression and combining statistical hypotheses and methods. Nucleic acids research **41**, 4378-4391.

17

Supplementary Figures

Supplementary Figure 1 [this file, see below]. Total nicotine metabolites in urine and carboxyhemoglobin (HbCO) levels in the study groups. (A) Total urine metabolites for the C57BL/6 study. Five representative nicotine metabolites (cotinine, norcotinine, nornicotine, nicotine-N'-oxide, and trans-3'-hydroxycotinine) were determined after 1,3 diethyl-2-thiobarbituric acid derivatization as described previously (Rustemeier et al., 1993) and their amounts were totaled. (B) Total urine metabolites in the Apoe$^{-/-}$ study. (C) Carboxyhemoglobin (HbCO) levels in blood in the C57BL/6 study. The uptake of aerosol components was monitored by measuring COHb levels in the peripheral blood, as previously described (Terpstra et al., 2003). (D) Carboxyhemoglobin levels in blood in the Apoe$^{-/-}$ study.

Supplementary Figure 2 [this file, see below]. Effect of cigarette smoke exposure, potential MRTP aerosol exposure, cessation, and switching to an MRTP on the lung lipidome of C57BL/6 and Apoe-/- mice. Differential abundance of lipid species was detected in both studies. These data are expressed as described for Figure 1E/F, but all lipid species that demonstrated significantly different abundance in any study and in any exposure group are included.

Supplementary Figure 3 [this file, see below]. Functional association clustering for the main sPLS-can component. (A) Identified clusters for the positively contributing proteins. (B) Identified clusters for the negatively contributing proteins. (C) Cluster expression profiles for the positively contributing proteins. The signed log10 adjusted p-value is color coded. (D) Cluster expression profiles for the negatively contributing proteins. The signed log10 adjusted p-value is color coded.

19

Supplementary Tables

Supplementary Table 1. Comparative analytical specifications of the pMRTP aerosol, THS2.2 aerosol, and 3R4F CS yields. Quantification of 56 HPHCs plus water and glycerol (as a humectant) in a total of 58 analytes from 3R4F CS and THS2.2 and pMRTP aerosols. All values in reference to nicotine content. Units are shown for each group of components)
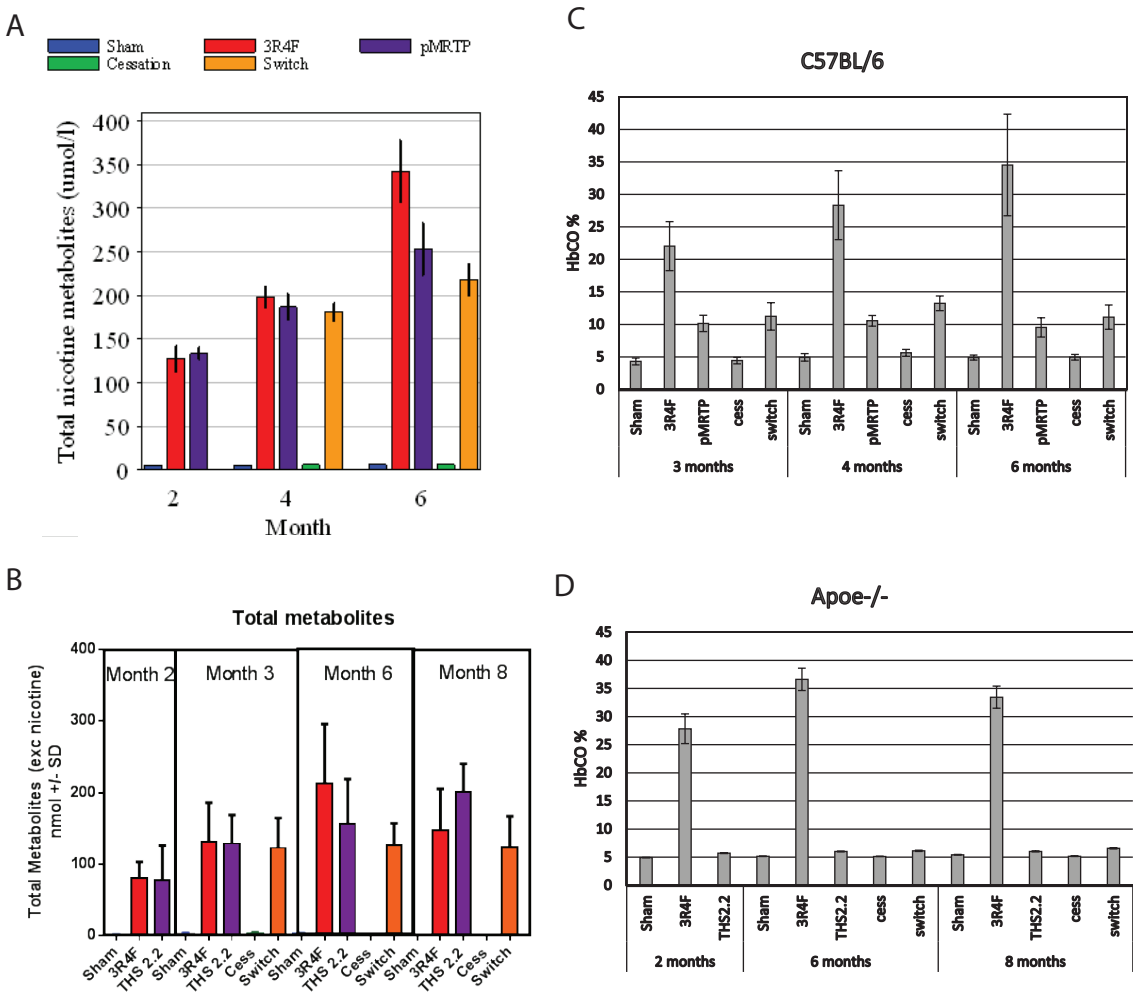
ISO parameters	pMRTP	THS2.2	3R4F
puff count **(mg/mg nicotine)**			
1. **Carbon monoxide**	2.58 ± 0.475	0.437 ± 0.031	14.8 ± 0.715
2. **Nicotine**	1 ± 0.101	1 ± 0.045	1 ± 0.0542
3. **Tar**	6.88 ± 1.6	6.304 ± 1.214	14.3 ± 0.717
4. **TPM**	35.6 ± 1.33	34.72 ± 1.396	22.2 ± 1.2
5. **Water**	27.8 ± 1.37	27.41 ± 1.937	7.01 ± 0.673
Aliphatic dienes **(µg/mg nicotine)**			
6. **1,3-Butadiene**	4/4 < 0.688	0.298 ± 0.053	36.7 ± 3.6
7. **Isoprene**	1.51 ± 0.338	2.483 ± 0.335	427 ± 36.4
Carbonyls **(µg/mg nicotine)**			
8. **Acetaldehyde**	70.8 ± 10.1	157.9 ± 15.78	323 ± 11.9
9. **Acetone**	11.7 ± 2.44	29.35 ± 3.463	77 ± 5.51
10. **Acrolein**	8.38 ± 1.44	8.165 ± 1.189	719 ± 50.1
11. **Butyraldehyde**	6.76 ± 1.05	20.32 ± 2.024	41.7 ± 3.64
12. **Crotonaldehyde**	24/30 < 2.16	2.809 ± 0.333	40.5 ± 4.31
13. **Formaldehyde**	17.1 ± 2.81	2.623 ± 0.271	28.3 ± 3.48
14. **Methyl ethyl ketone**	20/30 < 2.34	5.986 ± 0.91	91.9 ± 5.79
15. **Propionaldehyde**	4.71 ± 0.853	11.75 ± 1.483	58.1 ± 2.68
Acid derivatives **(µg/mg nicotine)**			
16. **Acetamide**	2.15 ± 0.307	3.063 ± 0.283	7.17 ± 0.399
17. **Acrylamide**	1.11 ± 0.131	1.918 ± 0.188	2.03 ± 0.157
18. **Acrylonitrile**	4/4 < 0.0709	0.166 ± 0.013	14.4 ± 0.894
Epoxides			

20

(µg/mg nicotine)

19.	**Ethylene oxide**	0.0886 ± 0.0148	0.167 ± 0.011	12.9 ± 0.998
20.	**Propylene oxide**	0.0429 ± 0.00274	0.094 ± 0.008	0.723 ± 0.0234

Nitro compounds

21.	**Nitrobenzene**	N.D.	N.D.	N.D.

Aromatic Amines
(ng/mg nicotine)

22.	**1-Aminonaphthalene**	3/4 < 0.207	0.065 ± 0.007	9.95 ± 0.6
23.	**2-Aminonaphthalene**	0.0665 ± 0.00782	3/4 < 0.024	5.11 ± 0.186
24.	**3-Aminobiphenyl**	4/4 < 0.0509	0.043 ± 0.005	1.64 ± 0.213
25.	**4-Aminobiphenyl**	4/4 < 0.0216	4/4 < 0.032	1.31 ± 0.115
26.	**o-Toluidine**	1.05 ± 0.199	0.962 ± 0.076	43.5 ± 1.45
27.	**Benzidine**	N.D.	4/4 < 7E-4	N.D.

N-heterocyclic aromatics
(µg/mg nicotine)

28.	**Pyridine**	0.745 ± 0.077	6.343 ± 0.283	18 ± 0.833
29.	**Quinoline**	4/4 < 0.02	0.016 ± 0.001	0.273 ± 0.0276

Halogen compounds
(ng/mg nicotine)

30.	**Vinyl chloride**	2.22 ± 0.485	4/4 < 2.477	50.2 ± 2.75

Inorganic compounds
(µg/mg nicotine)

31.	**Ammonia**	17.9 ± 0.919	10.18 ± 0.611	19.4 ± 0.847
32.	**Hydrogen cyanide**	4/4 < 0.21	2.905 ± 0.201	215 ± 17.2
33.	**Nitric oxide**	31.2 ± 1.73	11.37 ± 0.521	218 ± 10.3
34.	**Nitrogen oxides**	31.7 ± 1.56	11.48 ± 0.516	240 ± 12.3

Monocyclic aromatics
(µg/mg nicotine)

35.	**Benzene**	1.14 ± 0.0576	0.538 ± 0.037	46.8 ± 1.7
36.	**Styrene**	0.122 ± 0.013	0.578 ± 0.048	11.9 ± 0.497
37.	**Toluene**	0.533 ± 0.0573	2.172 ± 0.231	97.8 ± 3.8

N-nitrosamines
(ng/mg nicotine)

38.	**N-Nitrosoanabasine (NAB)**	3.12 ± 0.41	4/4 < 2.173	18 ± 1.24
39.	**N-Nitrosoanatabine (NAT)**	26 ± 2.72	11.67 ± 1.224	173 ± 10.1

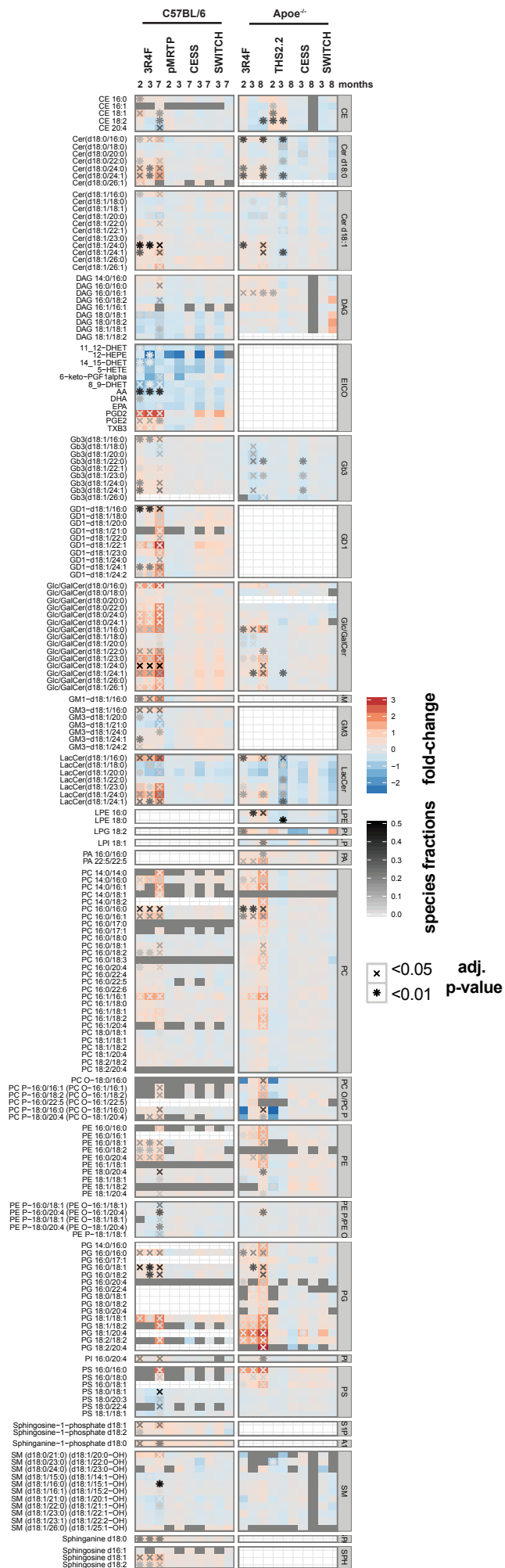|				
40.	4-(N-Nitrosomethylamino)-1-(3-pyridyl)-1-butanone (NNK)	13.5 ± 1.83	4.631 ± 0.387	117 ± 5.56
41.	N-Nitrosonornicotine (NNN)	16.9 ± 2.01	10.37 ± 1.039	155 ± 4.31

Phenols
(µg/mg nicotine)

42.	Catechol	8.62 ± 0.882	15.53 ± 1.698	43.8 ± 2.17
43.	m+p-Cresol	0.0393 ± 0.0173	0.123 ± 0.02	6.04 ± 0.448
44.	o-Cresol	0.0332 ± 0.013	0.102 ± 0.014	2.08 ± 0.18
45.	Hydroquinone	3.23 ± 0.316	6.614 ± 0.859	40.2 ± 1.85
46.	Phenol	0.463 ± 0.179	1.617 ± 0.269	6.59 ± 0.497
47.	Resorcinol	0.0148 ± 0.00149	0.049 ± 0.004	0.894 ± 0.0364

PAHs
(ng/mg nicotine)

48.	Benzo[a]pyrene	3.95 ± 0.27	3/4 < 0.696	4.66 ± 1.87
49.	Benz[a]anthracene	9.61 ± 0.533	1.078 ± 0.051	9.21 ± 3.19
50.	Dibenz[a,h]anthracene	0.362 ± 0.0479	4/4 < 0.07	3/8 < 0
51.	Pyrene	37.4 ± 1.76	4.085 ± 0.24	25.5 ± 15.2

Metals/Elements
(ng/mg nicotine)

52.	Arsenic	4.86 ± 0.36	3/3 < 0.787	3.32 ± 0.209
53.	Cadmium	4/4 < 0.54	0.371 ± 0.008	63.7 ± 3.28
54.	Chromium	2/4 < 0.848	3/3 < 0.118	4/4 < 0.257
55.	Lead	3/4 < 5.16	3/3 < 2.332	14.8 ± 0.773
56.	Mercury	0.813 ± 0.147	1.024 ± 0.105	1.86 ± 0.0981
57.	Nickel	3/4 < 0.848	2/3 < 0.118	4/4 < 0.257
58.	Selenium	4/4 < 0.848	3/3 < 0.383	0.687 ± 0.126

Supplementary Table 2 [separate xlsx file]. Raw lipid concentration measurements for the C57BL/6 and the Apoe$^{-/-}$ study.
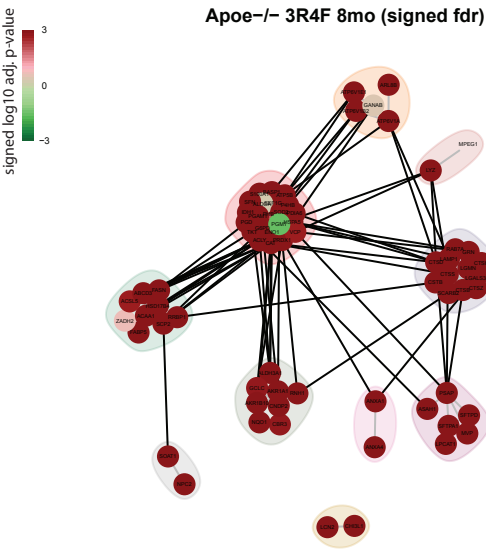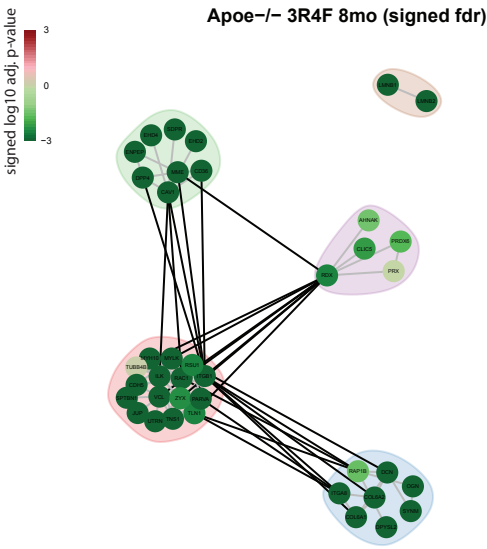
Supplementary Figure 1

A

B

C

D

Supplementary Figure 2

Supplementary Figure 3

A

Apoe−/− 3R4F 8mo (signed fdr)

B

Apoe−/− 3R4F 8mo (signed fdr)

C

D